

Polypyrrole based microwave absorbers

V.-T. TRUONG, S. Z. RIDDELL, R. F. MUSCAT

Aeronautical and Maritime Research Laboratory, Maritime Platforms Division, P.O. Box 4331 Melbourne, Victoria 3001 Australia
E-mail: tan.truong@dsto.defence.gov.au

Reflection of microwave radiations from single layer and two-layer materials is calculated. Microwave absorbing materials are formulated by mixing a commercially available paint or rubber with the conducting polypyrrole (PPy) powder. The reflection loss strongly depends on thickness and complex permittivity of the material. For a single layer material, optimum values of the real part, ϵ' , and imaginary part, ϵ'' , of the complex permittivity are found by calculations which lead to a minimum reflectivity at a given sample thickness. The ability to readily tailor the conductivity of the PPy powder enables the design of microwave absorbers according to theoretical desired values of ϵ' and ϵ'' . A paint panel containing 2 wt % of PPy powder with a thickness of 2.5 mm exhibits a reflectivity < -10 dB (i.e. at least 90% absorption of the incident radiation) over 12 to 18 GHz. Blending and milling during the manufacturing process can destroy the original fibrous shape of PPy aggregates leading to low radiation absorption. In an attempt to achieve a broadband absorber, a two-layer system consisting of a first layer containing PPy powder and a second layer containing carbonyl iron has been fabricated. © 1998 Kluwer Academic Publishers

1. Introduction

Carbon products behaving as dielectric loss materials, and carbonyl iron and ferrites functioning as magnetic loss materials are among the most popular conventional active components used in microwave radiation absorbers. Conducting polymers have emerged as a new class of materials in the last two decades. Because of their high conductivity, intriguing electrical properties and ease of production, potential applications such as microwave absorbers were seriously considered soon after the discovery of these materials [1]. However, perhaps due to the sensitivity of the subject there was a lapse of a decade before microwave absorption by conducting polymers has been discussed again in the open literature [2–4].

In this study, the design of polypyrrole based microwave absorbers based on theoretical calculations will be examined and compared with experimental results. The effect of manufacturing process on microwave properties will be discussed.

2. Materials and experimental

PPy powder was manufactured by a method described in a previous report [5] using freshly distilled pyrrole, FeCl_3 as an oxidant and 5-sulfosalicylic acid dihydrate (SSA) (Aldrich, 99%) or *p*-toluenesulfonic acid sodium salt (pTS) (Merck, >98%) as a codopant. The conductivity of the powder was varied between 0.01 and 30 S cm^{-1} by using different synthesis conditions. From the elemental analysis re-

sults, two typical empirical formulas of the PPy powders are $(\text{C}_4\text{H}_3\text{N})_5(\text{SSA})_1(\text{Fe})_{0.2}(\text{FeCl}_4^-)_{0.3}(\text{O})_{0.5}$ and $(\text{C}_4\text{H}_3\text{N})_{6.7}(\text{pTS})_1(\text{FeCl}_4^-)_{0.2}(\text{Cl}^-)_{0.3}(\text{O})_2$.

Paint panels were fabricated by mixing a commercial paint with a suitable quantity of PPy powder. The paint mixture was spread on an aluminium backing metal and the paint thickness was controlled within 10% of the required thickness. The paint was dried for at least 24 h prior to microwave measurements. Natural rubber was used as a matrix to fabricate a two-layer system. PPy powder or carbonyl iron was blended with the rubber with a mill at 60°C for 15 min. The blend was then moulded into a thin sheet of a required thickness by compressing at 140°C for 10 min.

Measurements of microwave radiation reflection were carried out on samples with the surface area of 15×15 cm and a thickness of 1 to 3 mm with a Hewlett-Packard 8510B Network Analyzer. All reflection measurements were obtained with the sample backed with an aluminium plate. The distance between the sample and the transmitting/receiving horns of the system was approximately 2.5 m which is regarded as a mid field range. The difference in reflectivity of a sample measured at mid field and that at far field is ± 1 dB [6]. The real and imaginary parts of the complex permittivity were measured with a coaxial cell and calculated from the reflection parameter, S_{11} , and the transmission parameter, S_{12} , according to Hewlett-Packard's standard procedures. Samples (2 to 3 mm thick) were fabricated into a doughnut shape to fit closely into a coaxial measurement cell. Teflon was used as a standard sample (5 mm thick).

3. Theoretical calculations

When an electromagnetic wave impinges on the surface of a material, the wave will undergo a combination of reflection, absorption and transmission. The exact behaviour of the electromagnetic wave at the surface and in the bulk of the material will critically depend on dielectric and magnetic properties of the material which are represented by the complex permittivity and complex permeability. The relative complex permeability, μ , and permittivity, ε , can be expressed by

$$\mu = \mu' - j\mu'' \quad (1)$$

$$\varepsilon = \varepsilon' - j\varepsilon'' \quad (2)$$

where $j = \sqrt{-1}$, ' and '' denote the real and imaginary parts, respectively. The voltage reflectivity of electromagnetic radiation, Γ , under normal wave incidence at the surface of a single-layer material backed by a perfect conductor (i.e. metal) can be expressed by [7, 8] (see Appendix)

$$\Gamma = \frac{\sqrt{\mu/\varepsilon} \tanh(\gamma d) - 1}{\sqrt{\mu/\varepsilon} \tanh(\gamma d) + 1} \quad (3)$$

and the power reflectivity, R (dB) is defined by

$$R = 20 \log_{10} |\Gamma| \quad (4)$$

where Γ is a complex number, $|\Gamma|$ is the modulus of Γ and d is the thickness of the sample. The constant γ is a complex propagation factor,

$$\gamma = j \frac{2\pi f}{c} \sqrt{\mu\varepsilon} \quad (5)$$

where f is the frequency and c is the propagating velocity of electromagnetic wave in vacuum.

In a two-layer model where Layer 1 is backed by a metal plate and Layer 2 is in contact with free space, Γ becomes (see Appendix)

$$\Gamma = \frac{\frac{\sqrt{\mu_1/\varepsilon_1} \tanh(\gamma_1 d_1) + \sqrt{\mu_2/\varepsilon_2} \tanh(\gamma_2 d_2)}{\sqrt{\mu_1\varepsilon_2/\mu_2\varepsilon_1} \tanh(\gamma_1 d_1) \tanh(\gamma_2 d_2) + 1} - 1}{\frac{\sqrt{\mu_1/\varepsilon_1} \tanh(\gamma_1 d_1) + \sqrt{\mu_2/\varepsilon_2} \tanh(\gamma_2 d_2)}{\sqrt{\mu_1\varepsilon_2/\mu_2\varepsilon_1} \tanh(\gamma_1 d_1) \tanh(\gamma_2 d_2) + 1} + 1} \quad (6)$$

where 1 and 2 denote the layer number.

4. Results and discussion

Fig. 1 shows the effect of the varying sample thickness on the calculated reflectivity of a non-magnetic material ($\mu' = 1$, $\mu'' = 0$). The position and intensity of the reflectivity peak is quite sensitive to the sample thickness. Experimental reflectivity follows the behaviour predicted by the theoretical calculation (Fig. 2) in which the reflection loss minima move toward low frequencies by typically as much as 7 GHz for every 1 mm increase in the material thickness.

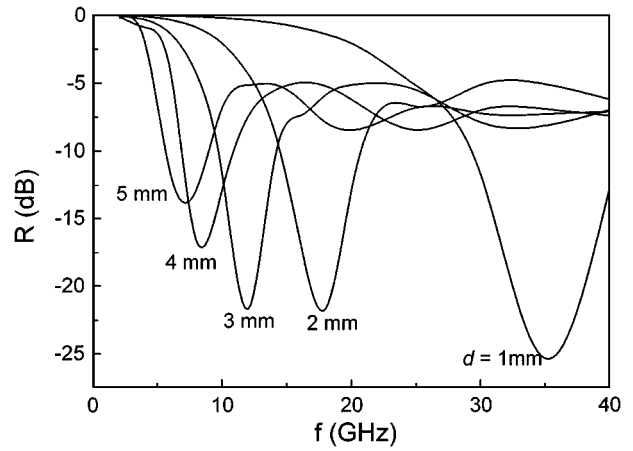


Figure 1 Calculation of the effect of thickness, d , on the reflection loss for a sample with $\varepsilon = 5 - j3$ and $\mu = 1 - j0$.

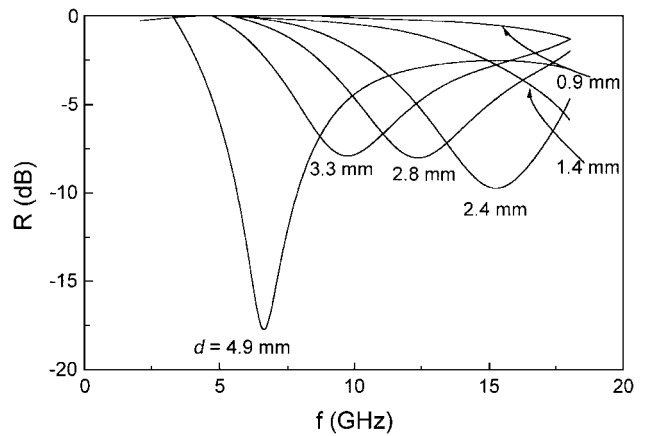


Figure 2 Effect of thickness, d , on the reflection loss of the paint containing milled PPy powder (2 wt %).

The propagating wavelength in the material, λ , is expressed by

$$\lambda = \frac{\lambda_0}{\sqrt{|\varepsilon||\mu|}} \quad (7)$$

where λ_0 is the wavelength in free space and $|\varepsilon|$ and $|\mu|$ are the modulus of ε and μ , respectively. The maximum reflection loss is customarily associated with a quarter wavelength (0.25λ) thickness of the material, but calculations can show a variation between 0.25λ and 0.3λ depending on the magnitude of $|\varepsilon|$ and $|\mu|$. Addition of a magnetic component can shift the peak to up to 0.5λ for the case where $|\mu| > |\varepsilon|$ [9].

Fig. 3 shows a comparison between the calculated values and the experimental results of a 2.5 mm thick paint panel containing PPy powder. The calculated results were obtained using the average values of 9 and 5 for ε' and ε'' , respectively. These values are averages obtained from the measurements of various PPy powder containing materials over the frequency range 2 to 18 GHz. The experimental curve agrees well with theoretical predictions, although the peak intensity is less and the position is 2 GHz lower than that of the calculated curve. These differences probably result from a combination of many factors including non-uniformity

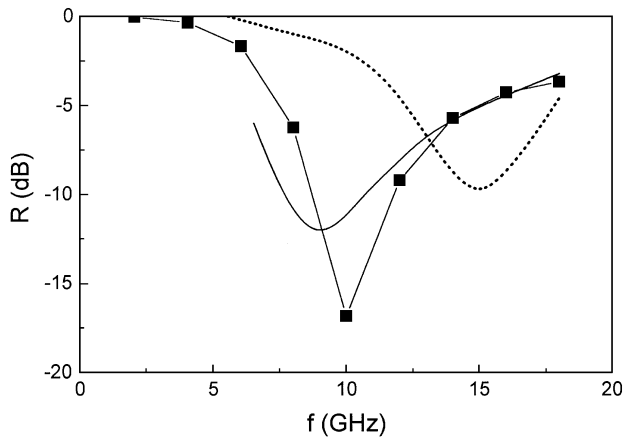


Figure 3 Comparison of calculated values and experimental results: (■) calculated results with $\epsilon = 9 - j5$, $\mu = 1 - j0$ and $d = 2.5$ mm; (—) paint with as-prepared unmilled PPy powder (2 wt %) and (....) paint with milled PPy powder (2 wt %).

of the sample thickness, non-planar wave incidence and dependence of ϵ' and ϵ'' on frequency.

The PPy aggregates prepared for this study exhibit a fibrous structure with an average length of $200 \mu\text{m}$ (Fig. 4). Consequently, a low percolation threshold (2–4 wt %) was obtained due to a high aspect ratio. During manufacturing processes involving mixing or blending, the rough fibrous texture of the PPy powder can be destroyed and lead to the formation of small spherical shape fillers (Fig. 4) which substantially increase the percolation threshold. This results in a greater quantity of filler required to achieve the desired dielectric properties, at the expense of mechanical properties. Therefore, if the powder is milled the original structure is broken down to a smaller spherical configuration, the percolation threshold increases to a value as high as 15.9% by volume [10]. This results in a decrease in ϵ' and ϵ'' of the paint containing milled PPy compared

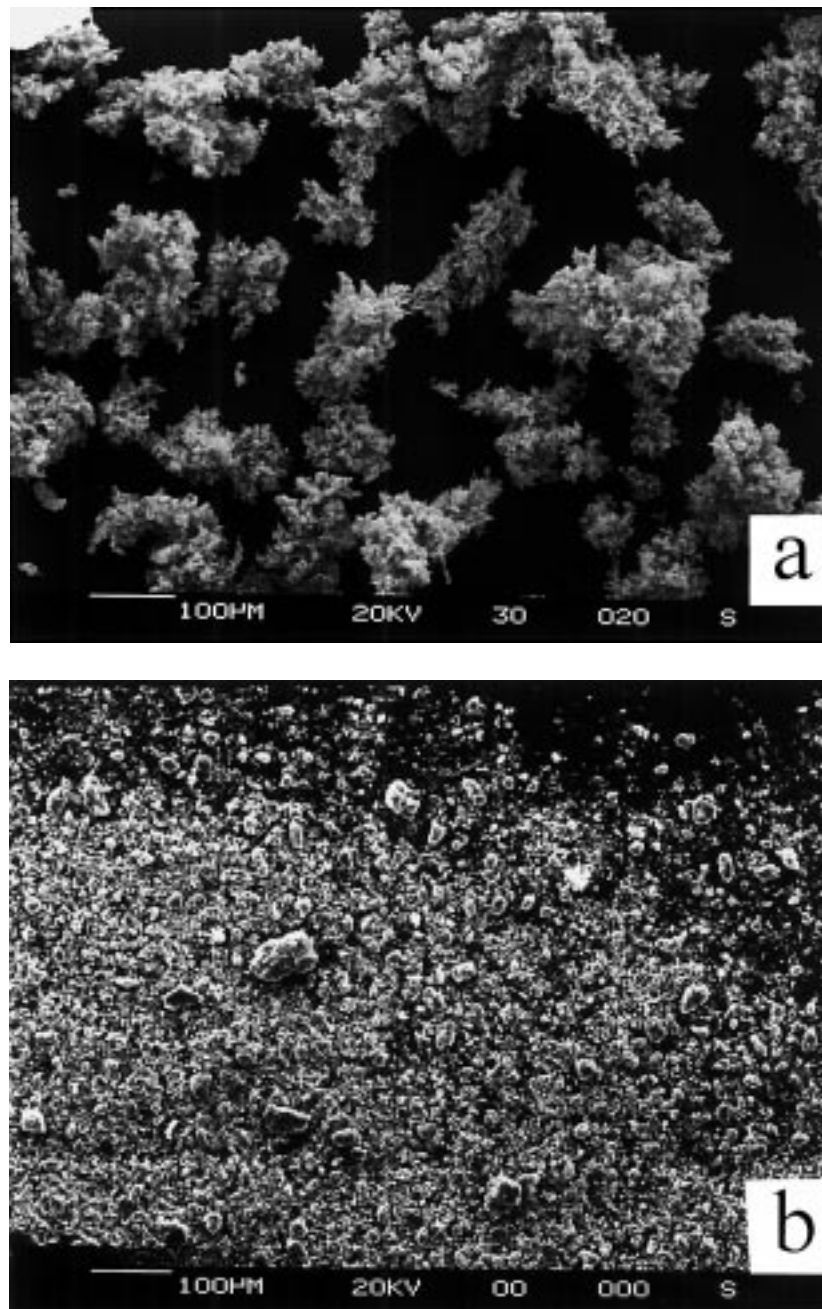


Figure 4 The geometrical shape of PPy powder: (a) as-prepared unmilled PPy and (b) milled PPy.

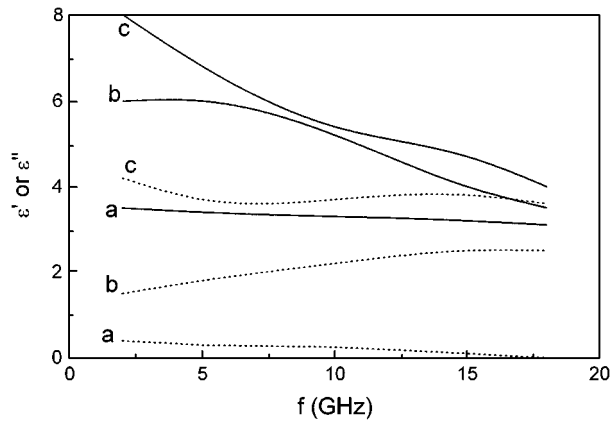


Figure 5 The real part, ϵ' (—), and the imaginary part, ϵ'' (.....), of the relative permittivity, ϵ , of paints: (a) paint only, (b) paint with milled PPy powder (2 wt %) and (c) paint with as-prepared unmilled PPy powder (2 wt %).

with the paint sample containing as-prepared unmilled PPy powder of the same content (Fig. 5). As shown in Fig. 3, the shift of the reflection peak to high frequency and the reduced intensity are a direct result of the low values of ϵ' and ϵ'' .

The imaginary part of the permittivity can be expressed by

$$\epsilon'' = \sigma_{dc}/\omega\epsilon_0 + \epsilon''_{ac} \quad (8)$$

where σ_{dc} is the dc conductivity, ω is the angular frequency, ϵ_0 is the permittivity of free space and ϵ''_{ac} is the loss contribution at high frequencies. Therefore, the measured value of ϵ'' consists of dc and ac factors. The ac loss contribution, ϵ''_{ac} , can be expressed by the Debye relaxation function [11] and described by the Cole-Cole diagram [12]. It is obvious that a high σ_{dc} is desirable for a high ϵ'' , but the ac contribution can be substantial even when the dc conductivity is low. It has been found that natural rubber containing PPy coated short fibres behaves as an insulator ($\sigma_{dc} \approx 0$), but exhibits a high value of ϵ'' ranging 0.5 to 5 at 10 GHz depending on the content of the fibres [13]. This reflects a high value of ϵ''_{ac} at microwave frequencies. On the other hand, since the physical shape of PPy powder aggregates is sensitive to mechanical forces in the blending process, when the PPy powder was blended with rubber at a content lower than the percolation threshold of 15.9% for spheres, ϵ'' was reduced to zero and the material became poorly absorbing. Olmedo *et al.* [3] have also pointed out that the values of ϵ' and ϵ'' are dependent on methods of fabrication which control the macroscopic morphology of the powder aggregates.

Fig. 6 shows the effect of varying ϵ' and ϵ'' on the intensity of the reflection loss peak. It is obvious that for a given thickness an optimum value of ϵ' and ϵ'' can be found to give the lowest reflectivity. Although the loss tangent has been customarily used as a parameter to measure the lossiness of materials, suitable values of ϵ' and ϵ'' should be selected to achieve a minimum reflectivity. The lowest reflectivity is obtained at $\epsilon' = 5$ and $\epsilon'' = 3$ for $d = 2.5$ mm. A paint containing PPy powder (2.5 mm thick) was fabricated with values of

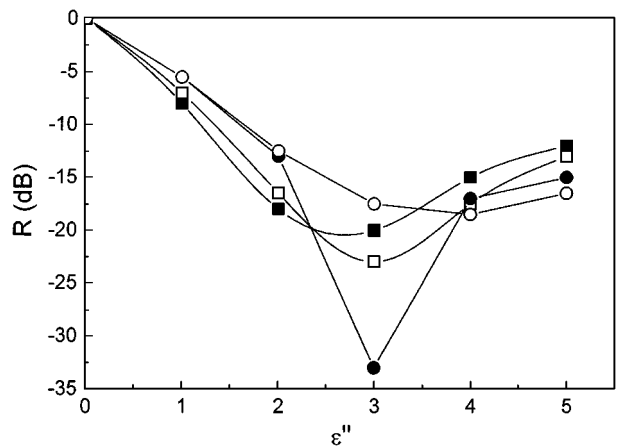


Figure 6 Calculation of the effect of ϵ' and ϵ'' on the reflection loss of a non-magnetic material ($d = 2.5$ mm). (■) $\epsilon' = 3$; (□) $\epsilon' = 4$; (○) $\epsilon' = 5$ and (●) $\epsilon' = 6$.

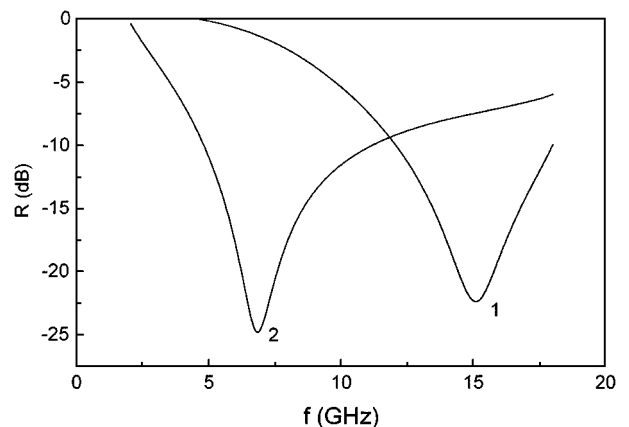


Figure 7 The reflection loss of the paints containing PPy powder only (curve 1, $d = 2.5$ mm), and containing a mixture of PPy powder (2 wt %) and carbonyl iron (ca. 25 % by volume) (curve 2, $d = 2.5$ mm).

ϵ' and ϵ'' tailored to give the lowest reflectivity. The paint provides a reflectivity < -10 dB over 12 to 18 GHz with a minimum reflection loss of -22 dB (curve 1 of Fig. 7). Compared with a multilayer ferrite loaded material 7.5 mm thick fabricated by Amin and James [14] and exhibiting a reflectivity < -10 dB over 5 to 18 GHz, this lightweight PPy based paint is easy to make and can be considered to be a thin absorber.

While materials with only dielectric loss component exhibit a narrow band absorption, those containing a combination of dielectric and magnetic active components show a broader absorption. Fig. 8 shows examples of the effect of varying the thickness and the relative permeability of a material containing dielectric/magnetic loss components calculated by Equation 3 using a typical value of μ' and μ'' ($\mu = 0.55 - j0.83$ [15] and $\mu = 1 - j1$ [16]). Although the thickness of this hypothetical hybrid material is 2 and 3 mm, there is no a large change in reflection loss. On the other hand, as shown in previous examples, materials involving dielectric loss only show significant variation in reflectivity with sample thickness (Figs 1 and 2). In practice, therefore, it is more convenient to manufacture materials with dielectric/magnetic loss where a high tolerance in thickness is acceptable, but where the weight

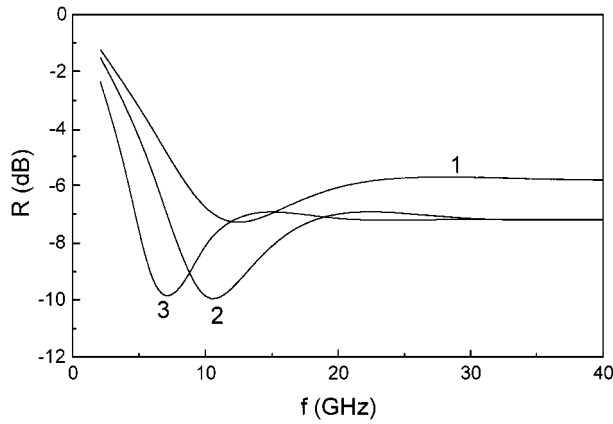


Figure 8 Calculated results for materials containing dielectric and magnetic loss fillers: (curve 1) $\epsilon = 8 - j4$, $\mu = 0.55 - j0.83$ and $d = 2$ mm; (curve 2) $\epsilon = 8 - j4$, $\mu = 1 - j1$ and $d = 2$ mm and (curve 3) $\epsilon = 8 - j4$, $\mu = 1 - j1$ and $d = 3$ mm.

and corrosion are undesirable trade-offs. Fig. 7 shows the reflectivity of samples with dielectric loss and with dielectric/magnetic loss. Incorporation of a magnetic component shifts the absorption peak to low frequencies as predicted by calculation, but the broadening effect is not observed. As the reflection curve is similar to that of material containing carbonyl iron only, the lack of broadening effect may be attributed to the masking of the dielectric component by a large quantity of carbonyl iron (ca. 25% by volume). A two-layer system consisting of a separate dielectric and magnetic layer may overcome the masking effect. The calculated results by Equation 6 are shown in Fig. 9. The two-layer rubber system was fabricated in order to compare the calculated results. The front layer (i.e. Layer 2 facing the incident radiations) contains carbonyl iron (ca. 25% by volume that gives $\epsilon = 8 - j0.5$, $\mu = 0.55 - j0.83$ [15]) and the back layer (Layer 1), which is intimately bonded to the front layer, contains PPy powder. The experimental data show a broadening effect and the agreement with the calculated results is acceptable.

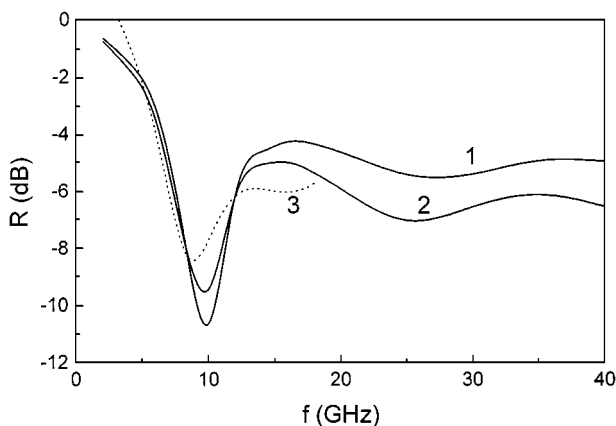


Figure 9 Comparison of the calculated examples and the experimental results for a two-layer system with Layer 1 containing dielectric loss filler and Layer 2 containing magnetic loss filler: (curve 1) Layer 1: $\epsilon = 5 - j3$, $\mu = 1 - j0$, $d = 2$ mm and Layer 2: $\epsilon = 8 - j0.5$, $\mu = 0.55 - j0.83$, $d = 1$ mm; (curve 2) Layer 1: $\epsilon = 5 - j3$, $\mu = 1 - j0$, $d = 2$ mm and Layer 2: $\epsilon = 8 - j0.5$, $\mu = 1 - j1$, $d = 1$ mm and (curve 3) experimental results obtained with a rubber specimen (see text).

5. Conclusions

The good agreement between the calculated and experimental results confirms the validity of employing theoretical calculations in designing microwave absorbing materials. By tailoring the conductivity of PPy, absorbing materials such as paints or rubbers containing a minimal amount of PPy based active fillers provide a suitable range of values of ϵ' and ϵ'' needed to obtain the lowest reflectivity. For these materials containing a relatively small amount (2 wt %) of PPy powder and typically 2.5 mm thick, a reflection loss of less than -10 dB over a bandwidth of 6 GHz can be realized. However, in designing a broadband absorber with a flat reflectivity curve, varying ϵ' and ϵ'' alone of PPy containing absorbing materials made little impact on broadness of the curve, while a combination of PPy powder and a magnetic loss component affords a more effective way to achieve broadband absorption.

Fragmentation of the PPy powder by mechanical forces during manufacturing processes can reduce ϵ' and ϵ'' . This is a disadvantage of the PPy powder. Since robustness of the active fillers is important in processing for a reproducible large scale production, tough materials with controllable dielectric loss are desirable. The shortcoming can be overcome by coating conducting polymers on tough short fibre glass or short flexible fibres. This merits further study.

Acknowledgements

The authors wish to thank Mr. A. Amiet for valuable assistance in measuring microwave reflectivity and transmission, and Mrs. M. S. Russo for technical assistance.

Appendix

For a single layer system, the incident impedance, Z_{in} , at free space and material interface is expressed by

$$Z_{in} = Z_0 \sqrt{\mu/\epsilon} \tanh(\gamma d) \quad (A1)$$

where Z_0 is the impedance of free space. The reflectivity is defined by

$$\Gamma = \frac{Z_{in} - Z_0}{Z_{in} + Z_0} \quad (A2)$$

Substituting Equation A1 into Equation A2 gives Equation 3. The reflectivity of a two-layer system, where Layer 1 is backed by a perfect conductor and Layer 2 is in contact with free space, is given by [7]

$$\Gamma = \frac{Z_{in2} - Z_0}{Z_{in2} + Z_0} \quad (A3)$$

where Z_{in2} is the incident impedance at free space and Layer 2 interface. Z_{in2} can be expressed by [7]

$$Z_{in2} = \frac{Z_{in1} + Z_2 \tanh(\gamma_2 d_2)}{(Z_{in1}/Z_2) \tanh(\gamma_2 d_2) + 1} \quad (A4)$$

where $Z_{in1} = Z_{in}$ (Equation A1)

$$Z_{in1} = Z_0 \sqrt{\mu_1/\varepsilon_1} \tanh(\gamma_1 d_1) \quad (\text{A5})$$

and Z_2 is the impedance of Layer 2

$$Z_2 = Z_0 \sqrt{\mu_2/\varepsilon_2} \quad (\text{A6})$$

Substituting Equations A4, A5 and A6 into Equation A3 gives Equation 6.

References

1. A. FELDBLUM, Y. W. PARK, A. J. HEEGER, A. G. MACDIARMID, G. WNEK, F. KARASZ and J. C. W. CHIEN, *J. Polym. Sci.: Polym. Phys. Ed.* **19** (1981) 173.
2. P. T. C. WONG, B. CHAMBERS, A. P. ANDERSON and P. V. WRIGHT, *Electronics Lett.* **28** (1992) 1651.
3. L. OLMEDO, P. HOURQUEBIE and F. JOUSSE, *Adv. Mater.* **5** (1993) 373.
4. P. HOURQUEBIE and L. OLMEDO, *Synth. Met.* **65** (1994) 19.
5. V.-T. TRUONG, DSTO Aeronautical and Maritime Research Laboratory, Internal Report, 1997.
6. A. AMIET, Defence Science and Technology Organisation, private communication.
7. P. G. LEDERER, "An Introduction to Radar Absorbent Materials" (Royal Signals and Radar Establishment, Malvern, UK), Report No. 85016, 1986.
8. Y. X. GAN, F. H. WANG and C. Q. CHEN, *Composites* **23** (1992) 435.
9. E. F. KNOTT, *IEEE Trans. Antennas Propag.* **AP-27** (1979) 698.
10. D. M. BIGG, in "Metal-Filled Polymers" edited by S. K. Bhattacharya (Marcel Dekker, New York, NY, 1986) p. 165.
11. C. CAMETTI, A. FURLANI, G. IUCCI and M. V. RUSSO, *Synth. Met.* **51** (1992) 45.
12. A. LIAN, S. BESNER and L. H. DAO, *Synth. Met.* **74** (1995) 21.
13. V.-T. TRUONG, unpublished results.
14. M. B. AMIN and J. R. JAMES, *The Radio and Electronic Engineering* **51** (1981) 209.
15. K. C. PITMAN, M. W. LINDLEY, D. SIMKIN and J. F. COOPER, *IEE Proc.-F*, **138** (1991) 223.
16. R. UENO, N. OGASAWARA and T. INUI, in "Ferrites: Proceedings of the International Conference" edited by H. Watanabe, S. Iida and M. Sugimoto (Japan, 1980) p. 890.

Received 28 October 1997

and accepted 18 September 1998